applied sciences

MDPI

Article

Synthesis, Molecular Docking, Druglikeness Analysis, and ADMET Prediction of the Chlorinated Ethanoanthracene Derivatives as Possible Antidepressant Agents

Mujeeb A. Sultan [1,*], Mansour S. A. Galil [2,3], Mohyeddine Al-Qubati [4,5], Mufeed M. Omar [1] and Assem Barakat [6,7,*]

1 Department of Pharmacy, Faculty of Medical Sciences, Aljanad University for Science and Technology, Taiz 6803, Yemen; mufeed.aa@just.ac
2 Chemistry Department, Faculty of Applied Sciences, Taiz University, Taiz 6803, Yemen; mansour0498@yahoo.com
3 Aljanad University for Science and Technology, Taiz 6803, Yemen
4 Department of Physics, Faculty of Applied Sciences, Taiz University, Taiz 6803, Yemen; Mohyeddine@just.ac
5 Faculty of Engineering and Information Technology, Aljanad University for Science and Technology, Taiz 6803, Yemen
6 Department of Chemistry, College of Science, King Saud University, Riyadh 11451, Saudi Arabia
7 Department of Chemistry, Faculty of Science, Alexandria University, Alexandria 21321, Egypt
* Correspondence: mujeeb.aa@just.ac (M.A.S.); ambarakat@ksu.edu.sa (A.B.); Tel.: +967-775873672 (M.A.S.); +966-11467-5901 (A.B.); Fax: +966-11467-5992 (A.B.)

Received: 22 September 2020; Accepted: 29 October 2020; Published: 31 October 2020

Abstract: Ethanoanthracene cycloadducts **(5–7)** ***anti*****, (5–7)** ***syn*****,** and **(5–7)** ***dec*** have been synthesized from the Diels–Alder (DA) reaction of diene 1,8-dichloroanthracene **2**, with the dienophiles; acrylonitrile **3**, 1-cynavinyl acetate **4,** and phenyl vinyl sulfone **5,** individually. The steric effect of dienophile substituents were more favorable toward the ***anti***-isomer formation as deduced from ^{1}H-NMR spectrum. The cheminformatics prediction for **(5–7)** ***anti*** and **(5–7)** ***syn*** was investigated. The in silico anticipated anti-depression activity of the **(5–7)** ***anti*** and **(5–7)** ***syn*** compounds were investigated and compared to maprotiline **9** as reference anti-depressant drug. The study showed that steric interactions play a crucial role in the binding affinity of these compounds to the representative models; 4xnx, 2QJU, and 3GWU. The pharmacokinetic and drug-like properties of **(5–7)** ***anti*** and **(5–7)** ***syn*** exhibited that these compounds could be represented as potential candidates for further development into antidepressant-like agents.

Keywords: anthracenes; Diels-Alder; ADMET prediction; pharmacokinetic; druglikeness; antidepressant

1. Introduction

Anthracenes are known scaffold due to their versatile applications, including pharmaceutical drugs [1–9] and molecular sensors [10]. Anthracenes, as a core structure, are explored in many transformations, due to more electrons, with the largest coefficients at C9/C10 [11–14]. Building an ethano-bridge on the central ring of anthracenes is an attractive approach, and ethanoanthracenes are of significant interest in the context of drug discovery of anticancer [5,6], antimalarial [15,16], and antidepressant agents, as well as in overcoming drug resistance in multi-drug resistant cancers [17–19].

Diels–Alder (DA) reaction [20], for which German chemists Diels and Alder were awarded the Nobel Prize in chemistry in 1950, is one of the most useful synthetic approaches for building ethanoanthracenes [21–23]. For example, maprotiline is a selective norepinephrine reuptake

inhibitor (sNRI), and was conventionally synthesized by Wilhelm et al., where the key step was the DA reaction of ethylene as dienophile to 9-substitutedanthracene precursor under high pressure (50 bar) and high temperature (150 °C) [24]. Later, many DA reactions have been developed using ethylene-equivalent dienophiles, such as phenyl vinyl sulfone [25–29], acrolein [18,30], nitroethylene [31,32], vinyldihaloborane [33], and vinyl phenyl sulfoxide [34]. The steric effect was found to play a major role on the regioselectivity of the DA reaction of 10-allyl-1,8-dichloroanthracene with 2-chloroacrylonitrile, 1-cyanovinyl acetate, and phenyl vinyl sulfone [25].

The cheminformatic tools, including the Prediction of Activity Spectra for Substances (PASS), Lipinski's rule of five, predictions of absorption, distribution, metabolism, excretion, and toxicity (ADMET) are useful applications for the optimization and well-targeting of chemical synthesis, biological testing, and drug discovery [35–37]. Molecular docking is another cheminformatics technique that is based on the energy scoring function in order to identify the most energetically favorable ligand conformation when bound with the active site of the target [38]. The general hypothesis is that lower energy scores represent better protein–ligand bindings compared to higher energy values [38,39]. The amine transporters regulate the neurotransmitter concentrations and play a role in mood and behavior disorders. These transporters are well known as targets for a broad range of antidepressant drugs, which are selective as norepinephrine reuptake inhibitors (sNRIs). Although the crystal structure of the human norepinephrine transporter (hNET) has not been reported yet, to understand the mechanism of action of norepinephrine reuptake inhibitors (NRIs), several attempts have been conducted by employing the homolog crystalized structures of the bacterial and invertebrate [40–42]. To design and discover new compounds could be work, as antidepressant-like agents are a challenge. Recently, we reported the DA reaction of 1,8-dichloroanthracene **2** and 2-chloroacrylonitrile under xylene reflux, affording two regioisomers [43]. To an extent, based on our research and the finding mention above, the microwave-assisted synthesis of new DA adduct ethanoanthracenes are reported, and the dienophile substituent effects on DA regioselectivity are described. In addition, the physiochemical properties, pharmacokinetics parameters, and biological activities of these adducts are theoretically investigated, in-depth. The docking of the compounds and maprotiline to the target models Drosophila model 4xnx [44], Bacterial Model 2QJU [45], and Bacterial Model 3GWU [46] were run, and the binding affinity was recorded as MolDock score function.

2. Materials and Methods

2.1. Synthesis

2.1.1. Synthesis of 4,5-Dichloro-9,10-dihydro-9,10-ethanoanthracene-12-carbonitrile **5** ***anti***, 1,8-Dichloro-9,10-dihydro-9,10-ethanoanthracene-12-carbonitrile **5** ***syn***, and 9,10-Dihydro-9,10-ethanoanthracene-12-carbonitrile **5** ***dec***

A solution of 1,8-dichloroanthracene **1** (200 mg, 0.8 mmol) and acrylonitrile **2** (200 µL, 3 mmol) in (1 mL) xylene was added into a 10 mL microwave reaction tube containing a stir bar. This tube was taken into the Microwave CEM Discover SP system after sealing with a plastic septum. The reaction was stirred for 40 h (4 times, 10 h per each) at 150 °C temperature, with power at 250 W and pressure of 17 psi as a default setting. After removing the solvent via a rotary evaporator, the NMR of the residue was recorded. ^{1}H-NMR ($CDCl_3$, JEOL 400 MHz): δ = 1.95–2.01 (m, 1H, CH(H-12, H-12′, H-12″)), 2.17–2.26 (m, 1H, CH(H-12, H-12′, H-12″)), 2.90–2.95 (m, 1H, CH(H-11, H-11′, H-11″)), 4.39 (t, J = 3.2 Hz, 0.18H, H-9″), 4.44 (t, J = 2.8 Hz, 0.26H, H-9′), 4.57 (d, J = 2.4 Hz, 0.18H, H-10″), 4.60 (d, J = 3.2 Hz, 0.56H, H-10), 5.46 (t, J = 2.4 Hz, 0.56H, H-9), 5.71 (d, J = 2.8 Hz, 0.26H, H-10′), 7.07–7.42 (m, 6.36H).

2.1.2. Synthesis of 4,5-Dichloro-12-cyano-9,10-dihydro-9,10-ethanoanthracen-12-yl Acetate **6** ***anti***, 1,8-Dichloro-12-cyano-9,10-dihydro-9,10-ethanoanthracen-12-yl Acetate **6** ***syn***, and 12-Cyano-9,10-dihydro-9,10-ethanoanthracen-12-yl Acetate **6** ***dec***

A solution of 1,8-dichloroanthracene **1** (1.2 g, 5 mmol) and 1-cyanovinyl acetate **3** (1.5 mL, 14 mmol) in (5 mL) xylene was refluxed at 150 °C for 48 h. After removing the solvent via a rotary evaporator, the isomers mixture was separated on thick TLC with the eluent system ethyl acetate: petroleum ether (1:10). For **6** ***anti***: ^{1}H-NMR ($CDCl_3$, JEOL 400 MHz): δ = 1.92(m,3H), 2.65(dd, J = 2.8 Hz, 3.2, 2H), 5.12(s, 1H), 5.38(t, J = 2.8 Hz, 1H), 7.10–7.20 (m,2H), 7.24(s, 2H), 7.26(s,1H), 7.37(d, J = 7.2 Hz, 1H); ^{13}C-NMR ($CDCl_3$, JEOL 100 MHz): δ = 20.63, 36.21, 41.93, 51.71, 72.50, 117.90, 124.44, 125.06, 127.73, 127.98, 128.11, 128.37,129.64, 129.81, 138.41, 138.53, 138.64, 139.52, 168.80 ppm. For **6** ***syn***: ^{1}H-NMR ($CDCl_3$, JEOL 400 MHz): δ = 1.97 (s, 3H), 2.03(dd, J = 2, 3.2 Hz, 1H), 2.70(dd, J = 3.2, 2.8 Hz, 1H), 4.41(t, J = 2.8 Hz, 1H), 6.09 (s, 1H), 7.14–7.26(m, 6H) ppm; ^{13}C-NMR ($CDCl_3$, JEOL 100 MHz): δ = 20.64, 42.96, 43.66, 44.83, 72.07, 117.76, 122.02, 122.17, 127.29, 127.66, 128.54, 128.98, 132.40, 132.52, 133.53, 133.80, 144.23, 144.43, 168.80 ppm. For **6** ***dec***: ^{1}H-NMR ($CDCl_3$, JEOL 400 MHz): δ = 1.90(s, 3H), 2.04(dd, J = 2.4, 3.2, 1H), 2.65(dd, J = 2.4, 2, 1H), 4.36(t, J = 2, 1H), 5.07(s, 1H), 7.12–7.31(m, 7H), 7.47–7.49(m, 1H) ppm; ^{13}C-NMR ($CDCl_3$, JEOL 100 MHz): δ = 20.68, 42.91, 43.72, 44.71, 7.20, 118.44, 123.42, 123.55, 125.96, 126.48, 127.25, 127.60, 128.50, 128.96, 136.34, 136.65, 141.96, 142.84, 169.01 ppm.

2.1.3. Synthesis of 4,5-Dichloro-12-(phenylsulfonyl)-9,10-dihydro-9,10-ethanoanthracene **7** ***anti***, 1,8-Dichloro-12-(phenylsulfonyl)-9,10-dihydro-9,10-ethanoanthracene **7** ***syn***, and 12-(Phenylsulfonyl)-9,10-dihydro-9,10-ethanoanthracene **7** ***dec***

A solution of 1,8-dichloroanthracene **1** (370 mg, 1.5 mmol) and phenyl vinyl sulfone **4** (302 mg, 2.4 mmol) in (3.5 mL) xylene was added into a 10-mL microwave reaction tube containing a stir bar. This tube was taken into the Microwave CEM Discover SP system after sealing with a plastic septum. The reaction was stirred for 40 h at 150 °C temperature, with power at 250 W and pressure at 17 psi as a default setting. After removing the solvent via a rotary evaporator, the NMR of the residue was recorded. ^{1}H-NMR ($CDCl_3$, JEOL 400 MHz): δ = 1.86–1.93 (m, 1H, CH(H-12, H-12′, H-12″)), 1.99–2.10 (m, 1H, CH(H-12, H-12′, H-12″)), 3.29–3.33 (m, 1H, CH(H-11, H-11′, H-11″)), 4.25 (t, J = 2.4 Hz, 0.11H, H-9″), 4.31 (t, J = 2.6 Hz, 0.18H, H-9′), 4.71 (d, J = 2.0 Hz, 0.11H, H-10″), 4.82 (d, J = 2.0 Hz, 0.71H, H-10), 5.31 (t, J = 2.6 Hz, 0.71H, H-9), 5.56 (broad s, 0.18H, H-10′), 6.89–7.29 (m, 11.22H).

2.1.4. Synthesis of 1,8-Dichloro-9,10-dihydro-9,10-ethanoanthracen-11-one **8**

To a solution of **6** ***anti*** (15 mg, 0.04 mmol) in THF (0.13 mL) and MeOH (26 µL), was added 14% aqueous KOH (0.1 mL). The mixture was stirred at 40 °C for 2 h then the temperature was increased to 60 °C. Water was added after cooling, then extracted with diethyl ether two times. The ether layer was combined, dried over $MgSO_4$ and filtered. The ether was evaporated to afford **8**, then NMR was recorded. ^{1}H-NMR ($CDCl_3$, JEOL 400 MHz): δ = 2.25 (d, J = 2.0 Hz, 2H), 4.74 (s, 1H), 5.53 (t, J = 2.4 Hz, 1H), 7.00 (t, J = 8.0 Hz, 2H), 7.16 (t, J = 8.4 Hz, 4H).

2.2. Cheminformatics Prediction

2.2.1. PASS Online

For all compounds and maprotiline, the structure was drawn using a ChemDraw software; ChemDraw® Ultra, version 12, 1986–2009, Cambridge Soft Corp, Akron, OH, USA. The structure was checked and cleaned up through pressing structure icon and saved as MDL Mol files (*.mol) to be ready for uploading into the PASS prediction website http://195.178.207.233/PASS/index.html (accessed on 15 April 2020). Then, the icon "predict activity" was pressed to give the predicted activities and their corresponding Pa values.

2.2.2. Molecular Docking

Preparation of the Compounds and Maprotiline

The preparation of the compounds **(5–7)** ***anti*****, (5–7)** ***syn*****, (5–7)** ***dec,*** and maprotiline **9** for docking studies is carried out as follows; the compound structure was drawn using ChemDraw Ultra 12/ Chem14 Pro 12 program, the structure was checked and cleaned up through pressing structure icon. The ACS document 1996 setting was selected by pressing file icon. The structure was copied and pasted into Chem14 Pro 12 window in order to obtain the 14 structures of the compound and to pre-optimize the compound with its function MM force field then saved as MOL File (.mol) format and thus being prepared for docking.

Preparation of the Protein Models

The crystal structures of hNET homology models with access protein data bank (PDB) codes 4xnx, 2QJU, and 3GWU were imported from the protein data bank (PDB; http://www.rcsb.org/pdb (accessed on 15 April 2020)) into the Molegro Virtual Docker (MVD 2013.6.0.0 (win32)) program individually. The structure was prepared through the pressing icon, and the errors in the amino acids, which appeared as a warning, were corrected. The protein surface and binding cavity were identified, respectively. After resetting the view from the view icon, the ligand that already binds in the binding site of the protein was removed, and the other ligands were converted to cofactors. The protein was ready for docking.

Docking of the Compounds into Protein Models

The previously optimized **(5–7)** ***anti*****, (5–7)** ***syn*****, (5–7)** ***dec,*** and maprotiline **9** were imported into the Molegro Virtual Docker (MVD 2013.6.0.0 (win32)) program containing pre-prepared protein. The docking wizard was selected, and then the program ran on a default setting. After finishing the run, the result file (in the left corner) was pressed, to open a new window containing poses of information and MolDock scores. The MolDock scores were recorded and the poses were visualized in Figures 1–3.

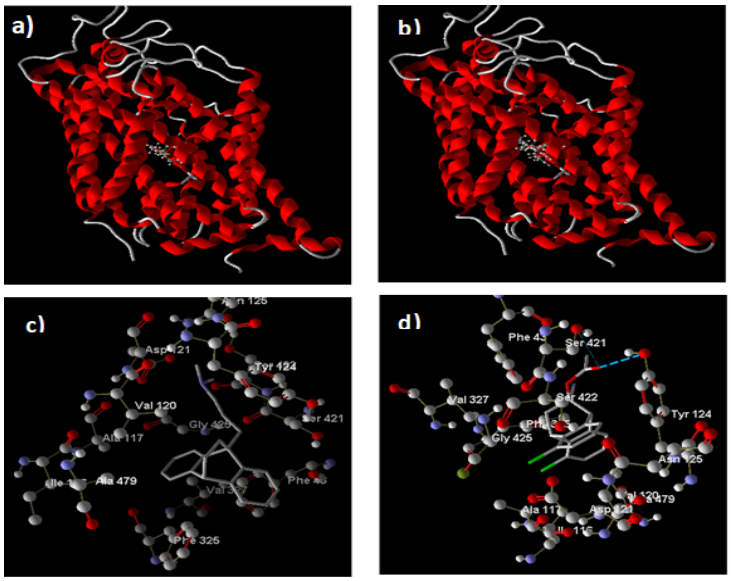

Figure 1. Structure of the **4xnx** model complex with: (**a**) its ligand, (**b**) **6** ***anti*** and reference drug maprotiline, (**c**) pose of reference drug maprotiline **9**, (**d**) pose of compound **6** ***anti.***

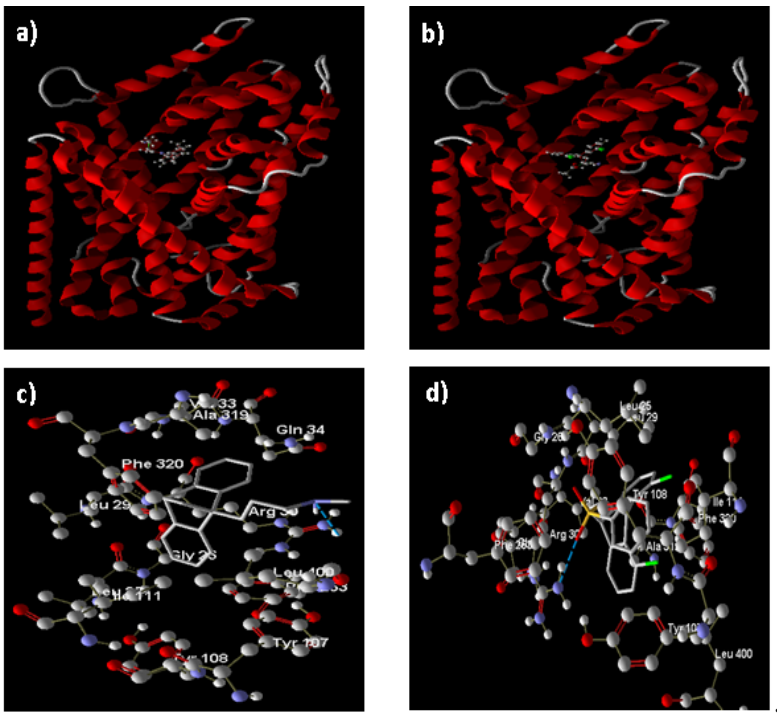

Figure 2. Structure of the **2QJU** model complex with: (**a**) its ligand DSM, (**b**) **6** ***Anti***, (**c**) pose of reference drug maprotiline **9**, (**d**) pose of compound **7** ***syn.***

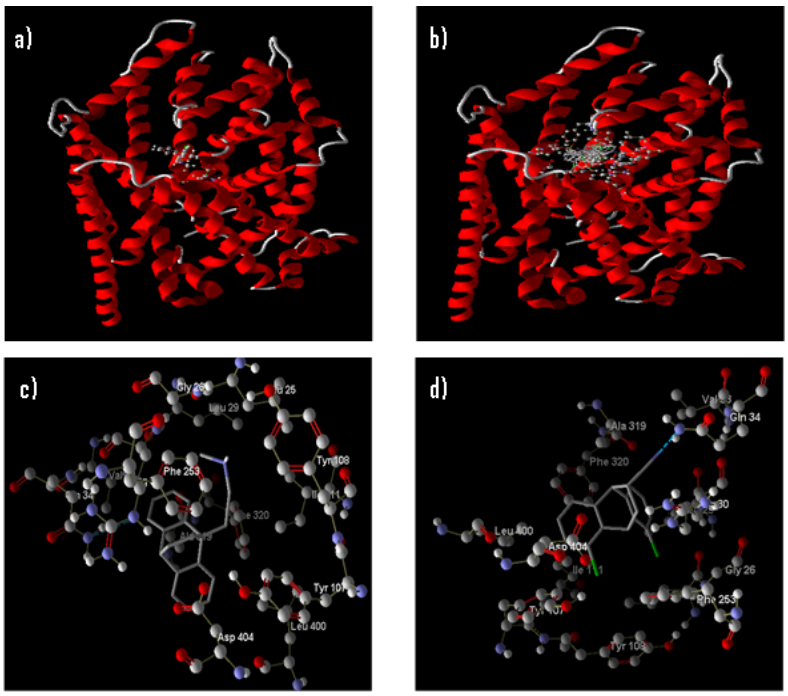

Figure 3. Structure of the **3GWU** model complex with: (**a**) its ligand sertraline, (**b**) all docked compounds **(5–7)** ***anti*** and **(5–7)** ***syn***, (**c**) Pose of maprotiline **9** as reference drug, (**d**) Pose of compound **5** ***anti***.

2.2.3. ADMET Prediction

For all compounds and maprotiline, the structure was drawn using ChemDraw software; ChemDraw® Ultra, version 12, 1986–2009, Cambridge Soft Corp., USA. The structure was checked and cleaned up through pressing the structure icon, saved as an MDL Mol file (*.mol), and were ready for

uploading into the SwissADME server; http://www.swissadme.ch/ (accessed on 15 April 2020). In the SwissADME server, the import icon in the molecular sketcher was clicked and a new window opened to select the prepared structure, presented on the molecular sketcher, then transferred this structure to the SMILES format. After that, the icon "Run" was pressed to give the ADMET parameters and related values.

3. Results and Discussion

3.1. Synthesis

The starting material 1,8-dichloroanthracene **1** was prepared in a good yield from commercially available 1,8-dichlroroanthraquinone, according to the House et al. procedure [47]. A literature survey revealed that 1,8-dichloroanthracene **1** is not reactive in DA reaction as anthracene itself. For example, del Rosario Benites et al. [48] reported the DA reaction between 1,8-dichloroanthracene **1** and phenyl vinyl sulfoxide; the reaction was under N_2 at chlorobenzene reflux (130 °C) and gave the cycloadduct in 30% yield after an 8-day reaction time, while Paquette et al. reported the successful DA reaction in 83% yield between the same dienophile and anthracene [34]. With the line of our interest on the DA reaction, 1,8-dichloroanthracene **1** reacted with acrylonitrile, 1-cynavinyl acetate, and phenyl vinyl sulfone to investigate the substituents effect in terms of regioselectivity. Initially, the reaction of phenyl vinyl sulfone—with 1,8-dichloroanthracene **1,** either in dichloromethane or toluene, under reflux conditions for 10 h—did not occur. Obviously, the reaction of 1,8-dichloroanthracene **1** with dienophiles is a challenge, and to get successful may be the reaction should be run under harsher conditions. An alternative way is to use the microwave-assisted organic synthesis technique because it has advantages compared to the conventional method, including being faster, safer, greener, more selective, and more economic [49–51]. This technique became an efficient tool in all organic reactions, including DA reaction [52,53]. We successfully synthesized the ethanoanthracenes via DA reaction with the microwave-assisted synthesis approach (Scheme 1).

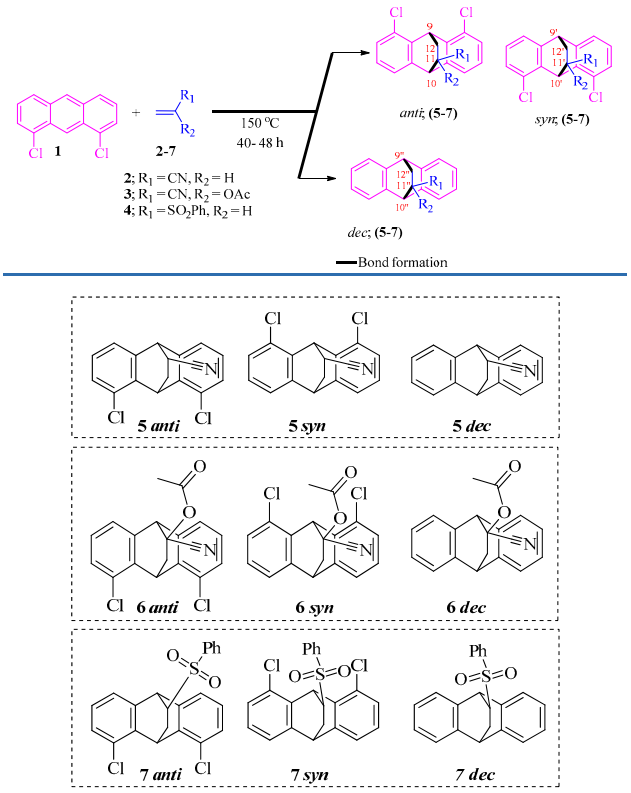

Scheme 1. Diels–Alder (DA) reactions of 1,8-dichloroanthracene **1** with dienophiles **2-4.**

The DA reactions of anthracenes with dienophiles, which lead to the possible formation of more than products, in terms of regioselectivity and stereoselectivity, have attracted the attention of more researchers. The effects of the substituent nature on the reaction of 2-substituted anthracenes with malic anhydride, affording two isomeric adducts, have been reported [54]. The substituent on the 1-position of anthracenes exerted a significant steric effect on the reaction stereoselectivity [55]. The steric factor of the substituent on the 1-position of 1-succinimidoanthracene and 1-phthalimidoanthracene was found to favor anti adduct formation [56]. On the other hand, when the substituent located in the 2-position postulated to have no steric effect as well, no major electronic effect could be explained in terms of the mechanism of the reaction [54]. However, the determination ratio of the two possible adducts was initiated as an approach to investigate the reaction mechanism [57]. Khan et al. reported that the amino group has an electronic effect on the isomer ratio when it is located in the 1- or 2-position of anthracene moiety [58]. In our pervious wok, the steric effect was found to play a major role on the regioselectivity of the DA reaction of 10-allyl-1,8-dichloroanthracene with 2-chloroacrylonitrile, 1-cyanovinyl acetate, and phenyl vinyl sulfone [25]. Recently, we reported the DA reaction of 1,8-dichloroanthracene **2** and 2-chloroacrylonitrile under xylene reflux for 48 h affording two regioisomers in a 2:1 ratio [43]. The synthetic route towards target regioisomers (**5–7**) ***anti*, (5–7)** ***syn*,** and **(5–7)** ***dec*** is shown in Scheme 1. As a result of the reaction, 1,8-dichloroanthracene **1** with acrylonitrile **2**, regioisomers **5** ***anti*, 5** ***syn***, and **5** ***dec*** were obtained as a mixture in a ratio 3.02:1.41:1, respectively (Supplementary Materials Figures S1 and S2). It sounds that the steric effect of the nitrile group, to chlorine atom, plays a crucial role in favor of regioisomer **5** ***anti***.

The NMR signals assigned to the bridge-head protons are usually utilized for isomer identification, and regioselectivity [5,16,18,19,25], (Table 1, Figure S2). It is clear that isomer **5** ***anti*** was the major cycloadduct, because the steric effect of the nitrile group (CN). The bridge-head proton H-9 of the isomer ***anti* 5** appeared at δ 5.46 ppm, which assigned, as triplet, with coupling constants *J* 2.4 Hz, on the other hand, the proton H-10 appeared at 4.60 ppm, as doublet, with coupling constants *J* 3.2 Hz, while the signal of the corresponding proton H-9′ of the isomer ***syn* 5** appeared at δ 4.44 ppm as triplet, with coupling constants *J* 2.8 Hz, and its signal assigned to the proton H-10′ appeared at δ 5.71 ppm, as doublet, with coupling constants *J* 2.8 Hz. Moreover, the signals assigned to the proton H-9″ of the dechlorinated isomer ***dec* 5** appeared at upfield δ 4.39 ppm, as triplet, with coupling constants J 3.2 Hz, and its signal assigned to the proton H-10″ appeared at δ 4.57 ppm, as doublet, with coupling constants *J* 2.4 Hz. The H-NMR signals of the unexpected dechlorination product **5** ***dec*** are well-matched to the signal of this compound, as reported in literature [59].

Table 1. The distinguishing between the isomers **5** ***anti***, **5** ***syn*,** and **5** ***dec*** using chemical shifts.

Isomer	Chemical Shift						Chemical Shift					
	H-9		H-9′		H-9″		H-10		H-10′		H-10″	
	δ	J	δ	J	δ	J	δ	J	δ	J	δ	J
5 ***anti***	5.46	t; 2.4					4.60	d; 3.2				
5 ***syn***			4.44	t; 2.8					5.71	t; 2.8		
5 ***dec***					4.39	t; 3.2					4.57	d; 2.4

The DA reaction of 1,8-dichloroanthracene **1** with 1-cynavinyl acetate **3** afforded **6** ***anti*, 6** ***syn*,** and **6** ***dec***. The steric effect of acetoxy substituent, beside the nitrile group on the dienophile, slightly increases the formation of regioisomer **6** ***anti***, since the ratio of **6** ***anti***: **6** ***syn***: **6** ***dec*** regioisomers is 2.7:1:2.5, respectively. In case of 10-allyl-1,8-dichloroanthracene, only anti isomer had been obtained when allowed 10-allyl-1,8-dichloroanthracene to react with the same dienophile 1-cyanovinyl acetate **3**. This may be attributed to the strong steric effect of the ally substituent [25]. Interestingly, the tracing of these isomers on TLC using the solvent system EA/PE 1:5 showed that R_f of **6** ***anti*** is the largest one and R_f of **6** ***dec*** is larger than **6** ***syn*** (Figure S3). After immersing this TLC in vanillin stain, the **6** ***anti*** and **6** ***syn*** exhibited yellow color, but **6** ***dec*** did not. However, the **6** ***dec*** spot was the most fluorescent

under the UV lamp. Furthermore, the migration of these compounds on the TLC plate was consistent with their chemical nature, as the **6** ***anti*** and **6** ***syn*** had two chlorine atoms, but the **6** ***dec*** did not. The NMR signals assigned to the bridge-head protons are presented in the Table 2. It is clear that isomer **6** ***anti*** is the major, because the steric effect resulted from the acetoxy ($OCOCH_3$) and nitrile (CN) groups. The bridge-head proton H-9 of the isomer ***anti*** **6** appeared at δ 5.12 ppm and assigned as singlet, on the other hands, the proton H-10 appeared at 5.38 ppm as triplet with coupling constants J 2.8 Hz, while the signal of the corresponding proton H-9′ of the isomer ***syn*** **6** appeared at δ 4.41 ppm, as triplet with coupling constants *J* 2.8Hz, indeed, the proton H-10′ appeared at δ 6.09 ppm as broad singlet, as well, the proton H-9″ of the dechlorinated isomer ***dec*** **7** appeared at upfield δ 4.36 ppm, as triplet, with coupling constants *J* 2.0Hz. Finally, the proton H-10″ appeared at δ 5.07 ppm as singlet. The upfield shifting of the H-9″ signals in the isomer ***dec*** **6**, comparison to the isomer ***anti*** **7**, may be attributed to the absence of chlorine atoms (Cl).

Table 2. The distinguishing between the isomers **6** ***anti***, **6** ***syn,*** and **6** ***dec*** using chemical shifts.

Isomer	Chemical Shift						Chemical Shift					
	H-9		H-9′		H-9″		H-10		H-10′		H-10″	
	δ	J	δ	J	δ	J	δ	J	δ	J	δ	J
6 ***anti***	5.38	t; 2.8					5.12	s				
6 ***syn***			4.41	t; 2.8					6.09	s		
6 ***dec***					4.36	t; 2					5.07	s

The DA reaction of 1,8-dichloroanthracene **1** with phenyl vinyl sulfone **4** gave the isomers; **7** ***anti,*** **7** ***syn,*** and **7** ***dec*** in a ratio 6.58:1.70:1, respectively, as deduced from NMR spectrum of their crude (Table 3, Figures S4 and S5). It is clear that isomer **7** ***anti*** is the major, because the steric effect resulted from the bulk phenyl sulfone group. In case of DA reaction of phenyl vinyl sulfone **4** with 10-allyl-1,8-dichloroanthracene, anti and syn isomers were obtained in a ratio 2:1 [25]. The increasing ratio of **7** ***syn*** may due to the steric hindrance of the phenyl group, and its close position to the allyl substituent that enforces the formation of the syn isomer in a more quantity than in case of 1,8-dichloroanthracene 1, where no allyl substituent [25]. The signal that assigned to bridge-head protons H-9 and H-10 of the isomer ***anti*** **7** appeared at chemical shifts δ 5.31 ppm, as triplet, and δ 4.82 ppm, as doublet, with coupling constants *J* 2 and 2.6 Hz, respectively, while the signal of the corresponding proton H-9′ of the isomer ***syn*** **7** appeared at chemical shift δ 4.31 ppm, as triplet, with coupling constants J 2.6, and its signal assigned to the proton H-10′ appeared at δ 5.56 ppm as broad singlet. Moreover, the signals assigned to the protons H-9′′ and H-10″ of the dechlorinated isomer ***dec*** **7** appeared at upfield chemical shifts δ 4.25 ppm, as triplet, and 4.71 ppm, as doublet, with coupling constants J 2.4 and 2 Hz, respectively. The upfield shifting of the H-9″ and H-10″ signals in the isomer ***dec*** **7**, comparison to the isomers ***anti*** **7** and ***syn*** **7**, may be attributed to the absence of chlorine atoms (Cl). The H-NMR signals assigned to the **7** ***dec*** is well-matched to the signals of this compound reported in the literature [26]. It is noteworthy to report, here, that the obtaining unexpected dechlorination products **5** ***dec,*** **6** ***dec,*** and **7** ***dec*** is establishing a new dechlorination method that could be utilized and developed in the field of removal of chlorinated aromatic pollutants.

Table 3. The distinguishing between the isomers **7** ***anti***, **7** ***syn,*** and **7** ***dec*** using chemical shifts.

Isomer	Chemical Shift						Chemical Shift					
	H-9		H-9′		H-9″		H-10		H-10′		H-10″	
	δ	J	δ	J	δ	J	δ	J	δ	J	δ	J
7 ***anti***	5.31	t; 2.6					4.82	d; 2				
7 ***syn***			4.31	t; 2.6					5.56	broad s		
7 ***dec***					4.25	t; 2.4					4.71	d; 2

The ketone **8** was obtained in a 100% yield from the hydrolysis of cycloadduct **6** ***anti***, using 14 % aqueous solution of KOH in THF/MeOH, (Scheme 2, Figures S6 and S7).

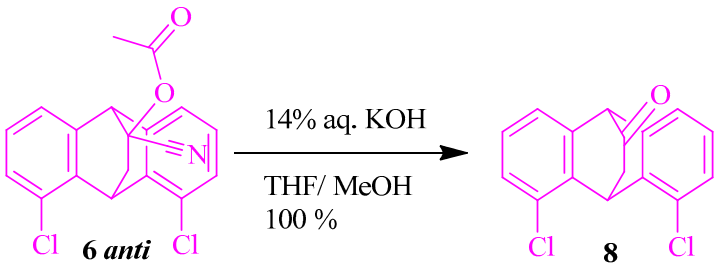

Scheme 2. Hydrolysis of cycloadduct **6** ***anti*** with aqueous KOH.

3.2. Cheminformatics Prediction

3.2.1. PASS Online

Prediction of Activity Spectra for Substances (PASS) is a free, online server designed for predicting the anticipated biological activities of the drug-like compounds (http://www.way2drug.com/passonline). This prediction is based on the structure–activity relationships (SAR) analysis of a library containing more than 300,000 organic compounds. Thus, PASS can be employed to optimize and well-target the chemical synthesis and biological testing [36]. The antidepressant and anti-phobic activities of the regioisomers (**5–7**) ***anti***, (**5–7**) ***syn*** and maprotiline **9**, as reference drug, were predicted, and the results are presented in Table 4. It is clear that compounds (**5–7**) ***anti*** and (**5–7**) ***syn*** could be recruited for the treatment of phobic disorders, as they have high predictive activity and are comparable to the maprotiline **9** (Pa: 0.842–0.877 for compounds (**5–7**) ***anti*** and (**5–7**) ***syn*** versus 0.897 for maprotiline **9**, but their antidepressant activity is lower than maprotiline **9** (Pa: 0.142–0.226 for compounds (**5–7**) ***anti*** and (**5–7**) ***syn*** versus 0.626 for maprotiline **9**.

Table 4. Prediction of antidepressant and anti-phobic activities of the compounds (**5–7**) ***anti***, (**5–7**) ***syn***, and maprotiline **9**.

Compound	Activity/Pa	
	Antidepressant	*Phobic Disorders Treatment*
5 ***anti***	0.226	0.877
5 ***syn***	0.226	0.877
6 ***anti***	0.142	0.875
6 ***syn***	0.142	0.875
7 ***anti***	0.169	0.842
7 ***syn***	0.169	0.842
Maprotiline 9	0.626	0.897

3.2.2. Molecular Docking

Docking of the Compounds (**5–7**) ***anti***, (**5–7**) ***syn***, and Maprotiline **9** into **4xnx** Model

The binding affinity of the compounds has been investigated and recoded as MolDock score (Table 5, Figure S8). The compound **7** ***syn*** has the highest MolDock score, −117.691, while compound **5** ***syn*** has the lowest MolDock, −89.0117, Table 5. In contrast to maprotiline, the compounds **5** ***anti***, **5** ***syn***, **6** ***syn***, **7** ***anti***, and **7** ***syn*** exhibit no hydrogen bond. Their binding with protein model is due to their steric interaction with the amino acids; Phe 325, Val 327, Asp 121, Val 120, Phe 43, Gly 425, Tyr 123, and Tyr 124. The compound **6** ***anti*** exhibits hydrogen bond with distance 3.09982 Å between its oxygen and nitrogen of Tyr 124, and maprotiline **9** exhibits hydrogen bond with distance 2.92323 Å between its nitrogen and amine oxygen of Ser 421, Figure 1.

Table 5. The interaction and MolDock scores of the docked compounds with three models: **4xnx, 2QJU,** and **3GWU.**

	4xnx Model			2QJU Model			3GWU Model		
Compound	**H- Bond (Length A)**	**Steric Interaction**	**MolDock Score**	**H- Bond (Length A)**	**Steric Interaction**	**MolDock Score**	**H- Bond (Length A)**	**Steric Interaction**	**MolDock Score**
5 ***anti***	-	Phe 325, Val 327, Asp 121, Val 120, Phe 43, Gly 425	−95.1957	-	Ile 111, Tyr 108, Phe 253, Leu 25, Arg 30, Leu 29, phe 320, Gly 26	−91.7484	Gln 34, (2.79245)	Leu 400, Tyr 107, Arg 30, Ala 319, Leu 29	−79.4448
5 ***syn***	-	Tyr 123, Tyr 124	−89.0117	-	Arg 30, Phe 320, Leu 29, Phe 253, Gly 26	−81.0802	-	Ala 319, Ile 111, Leu 400, Phe 320, Phe 253, Gln 34, Val 33	−82.7372
6 ***anti***	Tyr 124 (3.09982) Ser 421 (2.92323)	Ser 421, Gly 425, Phe 43, Phe 325	−103.964	Arg 30, (3.0999)	Arg 30, Tyr 107, Leu 400, Ala 319, Leu 29, Phe 320, Leu 25, Gly 26		-	Leu 400, Phe 320, Ala 319, Leu 29, Tyr 107, Tyr 108, Arg 30	−102.183
6 ***syn***	-	Asp 46, Phe 43, Phe 325	−102.65	-	Arg 30, Ala 319, Leu 400, Tyr 107, Phe 320, Asp 404, Phe 253, Val 33	−96.2236	-	Leu 400, Tyr 107, Ph 253, Gln 34, Ala 319, Phe 320	−93.9842
7 ***anti***	-	Tyr 124, Asp 46, Ala 44, Ser 320, Gly 322, Phe 43, Phe 325	−113.764	Arg 30, (2.74666)	Ala 319, Val 33, Phe 253, Tyr 108, Ile 111, Tyr 107, Arg 30, Asp 404, Phe 320, Leu 25, Leu 29	−103.8	-	Leu 25, Phe 320, Ala 319, Arg 30, Asp 404, Phe 253	−100.919
7 ***syn***	-	Phe 43, Phe 325, Tyr 124, Tyr 123, Gly 425, Phe 319	−117.691	Arg 30, (2.59754)	Phe 320, Ala 319, Tyr 107, Tyr 108, Ile 111, Phe 324, Leu 29, Leu 25, Arg 30, Phe 253, Gly 26	−96.6206	-	Ala 319, Leu 400, Asp 404, Arg 30	−104.221
Maprotiline 9	Asp 121, (3.24966)	Tyr 124, Asn 125, Ser 421, Asp 121	−95.561	Asp 404, (2.75112)	Arg 30, Asp 401, Asp 404, Phe 320	−99.2454	-	Arg 30, Ala 319	−91.4932

Docking of the Compounds (**5–7**) ***anti***, (**5–7**) ***syn***, and Maprotiline **9** into **2QJU** Model

The compound **7** ***anti*** has the highest MolDock score, −103.8, with hydrogen bond interaction (2.74666 Å) between its oxygen and the amine of Arg 30, while **5** ***syn*** has the lowest MolDock score, −81.0802, with no hydrogen bonding, Table 5. The amino acids Phe 320 and Arg 30 may play a significant role in the binding affinity, since they participate in the steric interactions of all docked compounds. Furthermore, Arg 30 participates in the hydrogen bonding with the two docked compounds; **6** ***anti*** and **7** ***syn***. Maprotiline exhibits hydrogen bond with distance 2.75112 Å between its nitrogen and oxygen of Asp 404, Figure 2. The other amino acids that affect the binding of the compounds are listed in Table 5.

Docking of the Compounds (**5–7**) ***anti***, (**5–7**) ***syn***, and Maprotiline **9** into **3GWU** Model

Although compound **7** ***syn*** has the highest MolDock score, −104.221, it has no hydrogen bond, while **5** ***anti*** has the lowest MolDock score, −79.4448, with hydrogen bond (2.79245 Å), Figure 3. The other docked compounds have no hydrogen bonding, so the hydrogen bonding is not more significant for enhancing binding affinity, (Table 5, Figure S9). The amino acid Ala 319 may play a major and significant role in the binding affinity, since it participates in the steric interaction of all docked compounds. As well, the amino acids Phe 320 and Arg 30 may play a significant role in the binding affinity, since they participate in the steric interaction of the most docked compounds. The others amino acids that affect the binding affinity of the compounds are listed in the Table 5. It is worthy, here, to mention that most of the amino acids that participate in the steric interaction of the compounds with the 3GWU model are the same or similar to those of the 2QJU model.

3.2.3. Drug-Likeness Prediction

Drug likeness is considered as a complex balance of molecular properties and structure merits that show the extent of similarity between certain compounds and known drugs. The drug likeness is guided by molecule properties, including hydrophobicity, electronic distribution, hydrogen bonding, molecule weight, pharmacophore entity, bioavailability, reactivity, toxicity, and metabolic stability [60]. Lipinski's rule is one of the tools most used to estimate the solubility and permeability of the compounds and, thus, to predict its qualification as a drug candidate. The rule states that: poor absorption or permeation is more likely when a compound violates Lipinski rule of 5; that it has more than 5 H-bond donors (the sum of NH and OH), molecular weight (MW_t) is over 500, Log P is over 5, and more than 10 H-bond acceptors (the sum of N and O) [61]. Table 6 depicts the drug likeness properties of the compounds **(5–7)** ***anti***, **(5–7)** ***syn,*** and maprotiline **9** using a free web SwissADME server; http://www.swissadme.ch/ [62]. All tested compounds **(5–7)** ***anti*****, (5–7)** ***syn,*** and maprotiline **9** as a reference drug do not violate Lipinski rule as their values fall in the normal range and the bioavailability shows that all compounds **(5–7)** ***anti*** and **(5–7)** ***syn*** are identical to the reference drug **9.** Furthermore, these compounds **(5–7)** ***anti*** and **(5–7)** ***syn*** are in the optimal range of the physiochemical space, as shown by the colored zone of the bioavailability radar and, thus, these compounds could be considered as lead compounds.

The pharmacokinetic parameters revealed that the tested compounds **5** ***anti***, **5** ***syn***, **6** ***anti,*** and **6** ***syn*** are similar to the reference drug maprotiline **9**, since they are highly absorbed through the gastrointestinal tract (GI) after oral intake, and able to penetrate through the blood–brain barrier (BBB), and could be effluxed by P-glycoprotein (P-gp), while compounds **7** ***anti*** and **7** ***syn*** are low absorbed through GI. This may be attributed to the molar refractivity (MR) of **7** ***anti*** and **7** ***syn,*** since it is higher than the MR of reference drug **9** (MR: 109.04 for **7** ***anti*** and **7** ***syn*** versus 88.32 for reference drug **9**), and even higher than MR values of other tested compounds.

The Brenk and pan assay interference compounds (PAINS) structural alerts have been used in medicinal chemistry to predict unstable, reactive, toxic fragments present in the structure [63,64]. All compounds **(5–7)** ***anti*** and **(5–7)** ***syn*** have zero alerts in Brenk and PAINS descriptors, providing other promising indicators to be drug candidates.

3.2.4. ADMET Prediction

The ADMET properties of the compounds **(5–7) *anti*, (5–7) *syn*,** and the reference drug maprotiline **9,** were predicted using ADMETlab server and the Data Warrior program, and the results were recorded in Tables 6 and 7. In term of absorption, all compounds **(5–7) *anti*** and **(5–7) *syn*** were found to have better membrane permeability (Caco-2) than reference drug **9**. The permeability glycoprotein (P-gp) is the most controlling drug efflux transporter; it shuttles drugs outside the cells, to the gut lumen, to urine from kidney, and outside the brain. The predicting efflux values reveal that all of the tested compounds, which are considered as antidepressants, are passing the central nervous system (CNS) drug efflux problem that leads to decrease their bioavailability. In more detail; the compounds **5 *anti***, **7 *anti*,** and **7 *syn*** are neither substrates nor inhibitors for P-gp, while the compounds **5 *syn***, **6 *anti*,** and **6 *syn*** are inhibitors, but not substrates that may help as synergic drugs. On the other hand, the reference drug **9** is inhibitor and substrate. Interestingly, the compounds **6 *anti*** and **6 *syn*** had greater probability as P-gp inhibitors than reference drug **9** (0.814, 0.839, and 0.558, respectively). The Human Intestinal Absorption (HIA) scores are coming in the line of qualitative gastrointestinal (GI) absorption descriptors, as predicted by SwissADME server, that the HIA scores of compounds **7 *anti*** and **7 *syn*** are less than the reference drug **9** score. In terms of distribution, three descriptors were measured; Plasma Protein Binding (PPB), Volume Distribution (VD), and Blood–Brain Barrier (BBB). In fact, there are three types of plasma protein that bind with drugs; human serum albumin, α- acid glycoprotein, and lipoprotein. The **6 *anti*** is the most one bound to the plasma protein followed by its isomer **6 *syn*** (PPP%: 93.528 and 93.448 respectively; versus, 87.029 of reference drug **9**), that is may refer to their acetoxy group ($OCOCH_3$) that increase their topological polar surface area (TPSA). In the same trend, the volume distribution (VD) results predict that compounds **6 *anti***, and **6 *syn*** are the most confined to blood components (VD: −0.331 and −0.323; respectively; versus, 1.603 of reference drug **9**), as well, the isomers **7 anti** and **7 syn** are strongly confined to blood. On the other hand, the isomers **5 *anti*** and **5 *syn*** were found to evenly distributed between blood and tissue components (VD: 0.581 and 0.604, respectively). All of the compounds could be penetrated through BBB. The **6 *anti*** and **6 *syn*** have the least BBB values (BBB: 0.915 for both; versus 0.984 for reference drug **9**). It is clear that acetoxy group ($OCOCH_3$) of the **6 *anti*** and **6 *syn*** raise up their TPSA and could participate in the hydrogen bonding that ultimately lead to decrease their penetration through BBB. This is in a good agreement with the Young et al. study where the excessive hydrogen bonding restricted the antihistamines penetration into the CNS [65]. In terms of metabolism, the compounds **(5–7) *anti*** and **(5–7) *syn*** could be metabolized by P450 CYP1A2 enzyme, so the lower affinity drugs to this enzyme are not preferred to intake with these compounds, as well, these compounds are not preferred to intake with reference drug **9,** since it has the highest affinity. In addition, only the **5 *anti*** and its isomer **5 *syn*** could behave as reversible and/or irreversible inhibitors for the P450 CYP1A2 enzyme and, thus, lead to reduce and/or diminish its activity. In the same manner, the compounds **(5–7) *anti*** and **(5–7) *syn*** could be metabolized by P450 CYP74, the enzyme responsible for biotransformation for about 30% of prescribed drugs [66]. The reference drug **9** could behave either as substrate or inhibitor for P450 CYP74 enzyme. The compounds **5 *anti***, **5 *syn***, **6 *anti***, **6 *syn***, and reference drug **9** are considered neither substrates nor inhibitors for the P450 CYP119 enzyme, while the **7 *anti*** and **7 *syn*** could behave either as substrates or inhibitors. The compounds **(5–7) *anti*** and **(5–7) *syn*** have a moderate half-life ($T_{1/2}$) time and low clearance rate (CL). The **5 *anti*** and its isomer **5 *syn*** have higher $T_{1/2}$ and CL, but reference drug **9** has the highest ($T_{1/2}$: 2.174, 2.34, and 3.401 h; CL: 1.424, 1.425, and 2.599 mL/min/kg, respectively).

Table 6. Physicochemical, pharmacokinetics, and medicinal chemistry properties of the compounds **(5–7) *anti*, (5–7) *syn*,** and Maprotiline **9** using SwissADME server.

Compound	MW (g/mol)	HBA	HBD	TPSA (Å^2)	Consensus Log Po/w *	MR	GI Absorption	BBB Permeant	P-gp Substrate	Lipinski	Bioavailability Score	PAINS (alert)	Brenk (alert)
5 *anti*	300.18	1	0	23.79	4.43	80.98	High	Yes	Yes	Yes **	0.55	0	0
5 *syn*	300.18	1	0	23.79	4.42	80.98	High	Yes	Yes	Yes **	0.55	0	0
6 *anti*	358.22	3	0	50.09	4.25	91.92	High	Yes	Yes	Yes	0.55	0	0
6 *syn*	358.22	3	0	50.09	4.22	91.92	High	Yes	Yes	Yes	0.55	0	0
7 *anti*	415.33	2	0	42.52	5.40	109.04	Low	No	No	Yes **	0.55	0	0
7 *syn*	415.33	2	0	42.52	5.38	109.04	Low	No	No	Yes **	0.55	0	0
Maprotiline 9	277.40	1	1	12.03	4.30	88.32	High	Yes	Yes	Yes **	0.55	0	0

MW: Molecular Weight; HBA: Num. H-Bond Acceptors; HBD: Num. H-Bond Donors; MR: Molar Refractivity; TPSA: Topological Polar Surface Area; P-M: Poor-Moderate; P: Poor; GI: Gastrointestinal; BBB: Blood–Brain Barrier; P-gp: P Glycoprotein; * Average of five prediction, ** 1 violation: MLOGP > 4.15, PAINS: Pan-assay Interference Compounds.

Table 7. ADME properties of the compounds **(5–7) *anti*, (5–7) *syn*,** and maprotiline **9** using ADMETlab server.

Compound	Absorption				Distribution			Metabolism; P450 CYP						Elimination	
	Caco-2 p (cm/s)	Pgp (I)	Pgp (S)	HIA	PPB%	VD (L/Kg)	BBB	1A2		74		119		$T_{\frac{1}{2}}$ h	CL mL/min/kg
								I	S	I	S	I	S		
5 *anti*	−4.402	−0.481	−0.036	++0.866	78.271	0.581	+++0.983	+0.568	+0.69	−0.243	+0.616	−0.331	−0.49	2.174	1.424
5 *syn*	−4.402	+0.521	−0.048	++0.866	77.559	0.604	+++0.983	++0.708	++0.754	−0.333	+0.648	−0.348	−0.452	2.34	1.425
6 *anti*	−4.479	++0.814	−0.008	++0.801	93.528	−0.331	+++0.915	−0.312	+0.576	−0.182	++0.7	−0.448	−0.444	2.059	0.647
6 *syn*	−4.472	++0.839	−0.004	++0.801	93.448	−0.323	+++0.915	−0.328	+0.674	−0.334	+0.684	−0.369	−0.473	2.065	0.613
7 *anti*	−4.496	−0.364	−0.04	++0.751	82.876	0.022	+++0.985	−0.141	+0.624	−0.258	+0.568	+0.613	+0.583	2.02	0.681
7 *syn*	−4.493	−0.384	−0.039	++0.751	82.776	0.042	+++0.985	−0.198	+0.68	−0.329	+0.6	+0.66	+0.597	2.112	0.659
Maprotiline 9	−4.387	+0.558	+0.511	++0.895	87.029	1.603	+++0.984	−0.086	+++0.938	++0.885	+0.612	−0.036	−0.281	3.401	2.599

PPB (Plasma Protein Binding); VD (Volume Distribution); BBB (Blood–Brain Barrier); $T_{1/2}$ (Half Life Time); CL (Clearance Rate); (I): Inhibitor; (S): Substrate.

Drug toxicology is one of the essential areas in the preclinical investigation, since the toxicity is a major factor leading for drug attrition at discovery and development phases [67]. Thus the in silico reliable prediction of compound toxicity is important in order to reduce expenses and to save a lot of time during the drug discovery and development [68]. The toxicity risk of the compounds **(5–7) *anti*** and **(5–7) *syn*,** and maprotiline **9,** was assessed quantitatively by ADMETlab server. Tables 7 and 8 and qualitatively by Data Warrior, a free tool from the marker of OSIRIS Property Explorer, Table 8.

Table 8. Toxicity risk assessment of the compounds **(5–7) *anti*, (5–7) *syn*,** and maprotiline **9** using Data Warrior and ADMETlab server *.

Compound	Mutagenicity	Tumorigenicity	Reproductive Effect	Irritating Effect	Toxicity *			
					hERG	H-HT	AMES	LD_{50} mg/kg
5 *anti*	None	None	None	None	−0.282	+0.564	+0.676	802.40
5 *syn*	None	None	None	None	−0.261	−0.414	+0.676	811.69
6 *anti*	High	None	High	High	++0.761	++0.756	−0.31	388.28
6 *syn*	High	None	High	High	++0.758	++0.774	−0.31	412.24
7 *anti*	None	None	None	None	+0.66	−0.484	−0.276	262.66
7 *syn*	None	None	None	None	+0.672	+0.508	−0.276	249.11
Maprotiline 9	None	None	High	None	++0.879	++0.878	−0.282	912.27

hERG: Human ether-à-go-go related gene; H-HT: Human Hepatotoxicity; AMES: Ames Mutagenicity; LD50: Median lethal dose; * calculated by ADMETlab server.

From a quantitative point of view, the four toxicity descriptors; cardiotoxicity, hepatotoxicity, Ames mutagenicity, and median lethal dose (LD_{50}) of acute toxicity were predicted. Cardiotoxicity is one of the side effects resulting from the off-target interactions between drugs and ion channels that play crucial roles in adjusting the cardiac action potential, as well as control the cardiac rhythm [69]. Among these ion channels, the human ether-a-go-go-related gene (hERG) a potassium ion channel, was found to be more related to severe cardiotoxicity [70,71], so the hERG-blockade is considered as a major retardant in providing the pharmaceutical market with safe drugs. Furthermore, the off-target interaction of hERG is the leading cause of drug withdrawal from the pharmaceutical market [72,73]. Thus, the identification of potential hERG blocker is important at early phases of drug discovery [69]. The assessment results of the hERG-based toxicity show that **5 *anti*** and its isomer **5 *syn*** have no cardiotoxicity and are the safest among other compounds. The highest cardiotoxicity value of the reference drugs **9** is, partially, at least, due to their containing basic amine on their alkyl side chain (hERG: ++ 0.879 for reference drugs **9** vs. — 0.261 for **5 *syn***). Hepatotoxicity and cardiotoxicity are the major factors participating for drugs attrition. Unfortunately, a quarter of the marketed drugs are withdrawn due to their adverse hepatic effects [74,75]. The **5 syn** and **7 *anti*** are safe to the liver, in contrast, **5 *anti*, 6 *anti*, 6 *syn*, 7 *syn*** are not safe. Furthermore, reference drug **9** is predicted to be the most hepatotoxic with probability ++ 0.878. The Ames test, referring to the inventor Ames, is an assay to detect the mutagenicity of the compound; the ability of the compound to stimulate the genetic damage and mutations [76,77]. Similar to reference drug **9**, the **6 *anti*, 6 *syn*, 7 *anti***, and **7 *syn*** exert no mutagenicity effects, while the **5 *anti*** and its isomer **5 *syn*** tend to induce genetic damage and mutations as predicted by Ames test. These results are not consistent with qualitative results obtained by the Data Warrior program, since **6 *anti*** and **6 *syn*** are highly mutagenic, while other compounds are not mutagenic. This may refer to the difference in the reference models used in both tests. Determination of an acute toxicity is another important task in the destination of drug discovery and development. The acute toxicity is expressed as median lethal dose (LD_{50}); the dose amount of a tested compound that kill fifty percent (50 %) of the treated animals within a given time [78]. The **7 *anti***, and its isomer **7 *syn*** exert the highest acute toxicity, and indicate their lowest LD_{50} values, while the reference drug **9** is safer due to the highest value (LD_{50} (mg/Kg): 262.66, 249.11, and 912.27, respectively). The **5 *anti*** and its isomer **5 *syn*** exhibit no acute toxicity with high LD_{50} 802.40, and 811.69 (mg/Kg), respectively, but the **6 *anti*** and its isomer **6 *syn*** may exert low toxicity.

From a qualitative point of view, the compounds **5** ***anti*****,** **5** ***syn*****,** **7** ***anti*****,** and **7** ***syn*** exhibit no mutagenicity, no tumorigenicity, no reproductive effect, and also have no irritability toxicity. The reference drug **9** shares with compounds **6** ***anti*** and **6** ***syn*** in their excreting reproductive toxicity. Furthermore, compounds **6** ***anti*** and **6** ***syn*** revealed mutagenicity and irritability toxicity

4. Conclusions

In conclusion, ethanoanthracene cycloadducts **(5–7)** ***anti*****,** **(5–7)** ***syn*****, and (5–7)** ***dec*** were synthesized, and the substituent effects on the regioselectivity of these cycloadducts were described. The antidepressant and anti-phobic activities of these cycloadducts **(5–7)** ***anti*****, (5–7)** ***syn*****,** and maprotiline **9** as a reference drug, were theoretically predicted through PASS and molecular docking. The PASS activity of the **(5–7)** ***anti*** and **(5–7)** ***syn*** against phobic disorders were high and comparable to maprotiline **9,** but variable and much less than maprotiline **9** as antidepressant. The MolDock scores of **(5–7)** ***anti*** and **(5–7)** ***syn*** are in the line with PASS values. The pharmacokinetic and druglikeness properties of **(5–7)** ***anti*** and **(5–7)** ***syn*** are valuable and provide an informative, promising analysis, as they are possible antidepressant-like compounds. Further in vitro and in vivo studies would be needed for confirmation of the chemoinformatics investigation.

Supplementary Materials: The following are available online at http://www.mdpi.com/2076-3417/10/21/7727/s1, Figure S1. Full ^{1}H-NMR spectrum of **5** ***anti*****,** **5** ***syn*** and **5** ***dec;*** Figure S2. Partial ^{1}H-NMR spectrum of **5** ***anti*****,** **5** ***syn*** and **5** ***dec;*** Figure S3. Schematic representation of the migration of **6** ***anti*****,** **6** ***syn*** and **6** ***dec*** on TLC; Figure S4. Full ^{1}H-NMR spectrum of **7** ***anti*****,** **7** ***syn*** and **7** ***dec;*** Figure S5. Partial ^{1}H-NMR spectrum of **7** ***anti*****,** **7** ***syn*** and **7** ***dec;*** Figure S6. Full ^{1}H-NMR spectrum of compound **8**; Figure S7. Partial ^{1}H-NMR spectrum of compound **8**; Figure S8. Structure of the **4xnx** model complex with the poses of compounds; Figure S9. Structure of the **3GWU** model complex with the poses of compounds

Author Contributions: Conceptualization, M.A.S. and A.B.; methodology, M.A.S., M.M.O., and A.B.; software, M.A.S., M.M.O., and A.B.; validation, A.B., A.M.A., M.S.A.G., and M.A.-Q.; formal analysis, A.B., and M.A.S.; investigation, A.B., M.A.S., A.M.A., M.S.A.G., and M.A.-Q.; resources, A.B., AM.A., M.S.A.G., and M.A-Q.; data curation, A.B., M.A.S., and M.A.-Q.; writing—original draft preparation, A.B. and M.A.S.; writing—review and editing, M.S.A.G. and M.A.-Q.; visualization, A.B., M.A.S., and M.M.O.; supervision, A.B., M.S.A.G., and M.A.-Q.; project administration, A.B., M.M.O., and M.A.S.; funding acquisition, A.B. All authors have read and agreed to the published version of the manuscript.

Funding: King Saud University-Researchers Supporting Project Number (RSP-2020/64).

Acknowledgments: The authors would like to extend their sincere appreciation to Researchers Supporting Project Number (RSP-2020/64), King Saud University, Riyadh, Saudi Arabia.

Conflicts of Interest: The authors declare no conflict of interest.

References

1. Lee, A.H.; Jang, Y.; Kim, G.H.; Kim, J.J.; Lee, S.S.; Ahn, B.J. Decolorizing an anthraquinone dye by Phlebia brevispora: Intra-species characterization. *Eng. Life Sci.* **2017**, *17*, 125–131. [CrossRef] [PubMed]
2. Xu, J.; Niu, G.; Wei, X.; Lan, M.; Zeng, L.; Kinsella, J.M.; Sheng, R. A family of multi-color anthracene carboxyimides: Synthesis, spectroscopic properties, solvatochromic fluorescence and bio-imaging application. *Dyes Pigment.* **2017**, *139*, 166–173. [CrossRef]
3. Wadler, S.; Fuks, J.Z.; Wiernik, P.H. Phase I and II agents in cancer therapy: I. Anthracyclines and related compounds. *J. Clin. Pharmacol.* **1986**, *26*, 491–509. [CrossRef] [PubMed]
4. Sunmonu, T.O.; Owolabi, O.D.; Oloyede, O.B. Anthracene-induced enzymatic changes as stress indicators in African catfish, Heterobranchus bidorsalis Geoffroy Saint Hilaire, 1809. *Res. J. Environ. Sci.* **2009**, *3*, 677–686.
5. McNamara, Y.; Bright, S.; Byrne, A.; Cloonan, S.; McCabe, T.; Williams, D.; Meegan, M. Synthesis and antiproliferative action of a novel series of maprotiline analogues. *Eur. J. Med. Chem.* **2014**, *71*, 333–353. [CrossRef]
6. Cloonan, S.M.; Drozgowska, A.; Fayne, D.; Williams, D.C. The antidepressants maprotiline and fluoxetine have potent selective antiproliferative effects against Burkitt lymphoma independently of the norepinephrine and serotonin transporters. *Leuk. Lymphoma* **2010**, *51*, 523–539. [CrossRef] [PubMed]

7. Cloonan, S.M.; Williams, D.C. The antidepressants maprotiline and fluoxetine induce Type II autophagic cell death in drug-resistant Burkitt's lymphoma. *Int. J. Cancer* **2011**, *128*, 1712–1723. [CrossRef]
8. Huang, H.-S.; Chiu, H.-F.; Hwang, J.-M.; JEN, Y.-M.; TAO, C.-W.; LEE, K.-Y.; LAI, Y.-L. Studies on anthracenes. 2. Synthesis and cytotoxic evaluation of 9-acyloxy 1, 8-dichloroanthracene derivatives. *Chem. Pharm. Bull.* **2001**, *49*, 1346–1348. [CrossRef]
9. Huang, H.-S.; Lin, P.-Y.; Hwang, J.-M.; TAO, C.-W.; Hsu, H.-C.; LAI, Y.-L. Studies on anthracenes. 3. Synthesis, lipid peroxidation and cytotoxic evaluation of 10-substituted 1, 5-dichloro-9 (10H)-anthracenone derivatives. *Chem. Pharm. Bull.* **2001**, *49*, 1288–1291. [CrossRef]
10. Bar, A.K.; Gole, B.; Ghosh, S.; Mukherjee, P.S. Self-assembly of a PdII neutral molecular rectangle via a new organometallic Pd II 2 molecular clip and oxygen donor linker. *Dalton Trans.* **2009**, 6701–6704. [CrossRef]
11. Phutdhawong, W.; Buddhasukh, D. Facile microwave-assisted synthesis of 9, 10-dihydro-9, 10-ethanoanthracene-11-carboxylic acid methyl ester. *Molecules* **2005**, *10*, 1409–1412. [CrossRef] [PubMed]
12. Atherton, J.; Jones, S. Diels–Alder reactions of anthracene, 9-substituted anthracenes and 9, 10-disubstituted anthracenes. *Tetrahedron* **2003**, *59*, 9039–9057. [CrossRef]
13. Wise, K.E.; Wheeler, R.A. Donor-acceptor-assisted Diels-Alder reaction of anthracene and tetracyanoethylene. *J. Phys. Chem. A* **1999**, *103*, 8279–8287. [CrossRef]
14. Hiruta, K.; Tokita, S.; Tachikawa, T.; Noguchi, F.; Nishimoto, K. Precise PPP molecular orbital calculations of excitation energies of polycyclic aromatic hydrocarbons. Part 6. 1 Spectrochemical atomic softness parameter. *J. Chem. Soc. Perkin Trans. 2* **2001**, 975–980. [CrossRef]
15. Bitonti, A.J.; Sjoerdsma, A.; McCann, P.P.; Kyle, D.E.; Oduola, A.; Rossan, R.N.; Milhous, W.K.; Davidson, D.E. Reversal of chloroquine resistance in malaria parasite Plasmodium falciparum by desipramine. *Science* **1988**, *242*, 1301–1303. [CrossRef] [PubMed]
16. Alibert, S.; Santelli-Rouvier, C.; Pradines, B.; Houdoin, C.; Parzy, D.; Karolak-Wojciechowska, J.; Barbe, J. Synthesis and Effects on Chloroquine Susceptibility in Plasmodium f alciparum of a Series of New Dihydroanthracene Derivatives. *J. Med. Chem.* **2002**, *45*, 3195–3209. [CrossRef] [PubMed]
17. Szabó, D.; Szabó, G.; Ocsovszki, I.; Aszalos, A.; Molnár, J. Anti-psychotic drugs reverse multidrug resistance of tumor cell lines and human AML cells ex-vivo. *Cancer Lett.* **1999**, *139*, 115–119. [CrossRef]
18. Karama, U.; Sultan, M.A.; Almansour, A.I.; El-Taher, K.E. Synthesis of chlorinated tetracyclic compounds and testing for their potential antidepressant effect in mice. *Molecules* **2016**, *21*, 61. [CrossRef]
19. Sultan, M.A.; Almansour, A.I.; Pillai, R.R.; Kumar, R.S.; Arumugam, N.; Armaković, S.; Armaković, S.J.; Soliman, S.M. Synthesis, theoretical studies and molecular docking of a novel chlorinated tetracyclic:(Z/E)-3-(1, 8-dichloro-9, 10-dihydro-9, 10-ethanoanthracen-11-yl) acrylaldehyde. *J. Mol. Struct.* **2017**, *1150*, 358–365. [CrossRef]
20. Diels, O.; Alder, K. Synthesen in der hydroaromatischen Reihe. *Justus Liebigs Ann. Chem.* **1928**, *460*, 98–122. [CrossRef]
21. Brocksom, T.J.; Nakamura, J.; Ferreira, M.L.; Brocksom, U. The Diels-Alder reaction: An update. *J. Braz. Chem. Soc.* **2001**, *12*, 597–622. [CrossRef]
22. Mehta, G.; Uma, R. Stereoelectronic Control in Diels− Alder Reaction of Dissymmetric 1, 3-Dienes. *Acc. Chem. Res.* **2000**, *33*, 278–286. [CrossRef] [PubMed]
23. Kanishchev, O.S.; Sanselme, M.; Bouillon, J.-P. Hetero-Diels–Alder reactions of perfluoroalkyl thioamides with electron-rich 1, 3-dienes: Synthesis of new 2-aminosubstituted-3, 6-dihydro-2H-thiopyrans and related compounds. *Tetrahedron* **2013**, *69*, 1322–1336. [CrossRef]
24. Wilhelm, M.; Schmidt, P. Synthese und Eigenschaften von 1-Aminoalkyl-dibenzo [b, e] bicyclo [2.2. 2] octadienen. *Helv. Chim. Acta* **1969**, *52*, 1385–1395. [CrossRef] [PubMed]
25. Sultan, M.A.; Karama, U. Substituent effects on regioselectivity of the Diels-Alder reactions: Reactions of 10-allyl-1, 8-dichloroanthracene with 2-chloroacrylonitrile, 1-cyanovinyl acetate and phenyl vinyl sulfone. *J. Chem.* **2016**, *34*, 1–5. [CrossRef]
26. Carr, R.V.; Williams, R.V.; Paquette, L.A. Dienophilic properties of phenyl vinyl sulfone and trans-1-(phenylsulfonyl)-2-(trimethylsilyl) ethylene. Their utilization as synthons for ethylene, 1-alkenes, acetylene, and monosubstituted alkynes in the construction of functionalized six-membered rings via [4+ 2]. pi. cycloaddition methodology. *J. Org. Chem.* **1983**, *48*, 4976–4986.

27. Dalai, S.; Belov, V.N.; Nizamov, S.; Rauch, K.; Finsinger, D.; de Meijere, A. Access to Variously Substituted 5, 6, 7, 8-Tetrahydro-3H-quinazolin-4-ones via Diels–Alder Adducts of Phenyl Vinyl Sulfone to Cyclobutene-Annelated Pyrimidinones. *Eur. J. Org. Chem.* **2006**, *2006*, 2753–2765. [CrossRef]
28. Omodani, T.; Shishido, K. Total enantioselective synthesis of the marine sesquiterpene nanaimoal. *J. Chem. Soc. Chem. Commun.* **1994**, 2781–2782. [CrossRef]
29. Bull, J.R.; Bischofberger, K. Cycloaddition of phenyl vinyl sulphone to 3-methoxy-16-methylestra-1, 3, 5 (10), 14, 16-pentaen-17-yl acetate: Synthesis of 14-functional ised 19-norpregnane derivatives. *J. Chem. Soc. Perki Trans. 1* **1991**, 2859–2865. [CrossRef]
30. Taarning, E.; Madsen, R. Unsaturated aldehydes as alkene equivalents in the Diels–Alder reaction. *Chem. -A Eur. J.* **2008**, *14*, 5638–5644. [CrossRef]
31. Ono, N.; Miyake, H.; Kamimura, A.; Kaji, A. Regioselective Diels–Alder reactions. The nitro group as a regiochemical control element. *J. Chem. Soc. Perkin Trans. 1* **1987**, 1929–1935. [CrossRef]
32. Wade, P.A.; Murray, J.K.; Shah-Patel, S.; Carroll, P.J. Generation and in situ Diels–Alder reactions of activated nitroethylene derivatives. *Tetrahedron Lett.* **2002**, *43*, 2585–2588. [CrossRef]
33. Zaidlewicz, M.; Binkul, J.R.; Sokół, W. Syntheses with organoboranes. IX. Vinyl-and 1-alkenyldichloroboranes as ethylene and 1-alkene equivalents for the Diels–Alder reaction. *J. Organomet. Chem.* **1999**, *580*, 354–362. [CrossRef]
34. Paquette, L.A.; Moerck, R.E.; Harirchian, B.; Magnus, P.D. Use of phenyl vinyl sulfoxide as an acetylene equivalent in Diels-Alder cycloadditions. *J. Am. Chem. Soc.* **1978**, *100*, 1597–1599. [CrossRef]
35. Alavijeh, M.S.; Chishty, M.; Qaiser, M.Z.; Palmer, A.M. Drug metabolism and pharmacokinetics, the blood-brain barrier, and central nervous system drug discovery. *NeuroRx* **2005**, *2*, 554–571. [CrossRef] [PubMed]
36. Filimonov, D.; Lagunin, A.; Gloriozova, T.; Rudik, A.; Druzhilovskii, D.; Pogodin, P.; Poroikov, V. Prediction of the biological activity spectra of organic compounds using the PASS online web resource. *Chem. Heterocycl. Compd.* **2014**, *50*, 444–457. [CrossRef]
37. Baldi, A. Computational approaches for drug design and discovery: An overview. *Syst. Rev. Pharm.* **2010**, *1*, 99. [CrossRef]
38. Thomsen, R.; Christensen, M.H. MolDock: A new technique for high-accuracy molecular docking. *J. Med. Chem.* **2006**, *49*, 3315–3321. [CrossRef] [PubMed]
39. Liu, Y.; Xu, Z.; Yang, Z.; Chen, K.; Zhu, W. A knowledge-based halogen bonding scoring function for predicting protein-ligand interactions. *J. Mol. Model.* **2013**, *19*, 5015–5030. [CrossRef]
40. Wang, H.; Goehring, A.; Wang, K.H.; Penmatsa, A.; Ressler, R.; Gouaux, E. Structural basis for action by diverse antidepressants on biogenic amine transporters. *Nature* **2013**, *503*, 141–145. [CrossRef]
41. Yamashita, A.; Singh, S.K.; Kawate, T.; Jin, Y.; Gouaux, E. Crystal structure of a bacterial homologue of Na+/Cl–dependent neurotransmitter transporters. *Nature* **2005**, *437*, 215–223.
42. Zheng, G.; Xue, W.; Wang, P.; Yang, F.; Li, B.; Li, X.; Li, Y.; Yao, X.; Zhu, F. Exploring the inhibitory mechanism of approved selective norepinephrine reuptake inhibitors and reboxetine enantiomers by molecular dynamics study. *Sci. Rep.* **2016**, *6*, 26883. [CrossRef]
43. Sultan, M.A.; Karama, U.; Almansour, A.I.; Soliman, S.M.; Ghabbour, H.A.; Mabkhot, Y.N. Synthesis, Characterization and DFT Calculations of 4, 5, 12-and 1, 8, 12-trichloro-9, 10-dihydro-9, 10-ethanoanthracene-12-carbonitriles. *Crystals* **2017**, *7*, 259. [CrossRef]
44. Penmatsa, A.; Wang, K.H.; Gouaux, E. X-ray structures of Drosophila dopamine transporter in complex with nisoxetine and reboxetine. *Nat. Struct. Mol. Biol.* **2015**, *22*, 506. [CrossRef]
45. Zhou, Z.; Zhen, J.; Karpowich, N.K.; Goetz, R.M.; Law, C.J.; Reith, M.E.; Wang, D.-N. LeuT-desipramine structure reveals how antidepressants block neurotransmitter reuptake. *Science* **2007**, *317*, 1390–1393. [CrossRef] [PubMed]
46. Zhou, Z.; Zhen, J.; Karpowich, N.K.; Law, C.J.; Reith, M.E.; Wang, D.-N. Antidepressant specificity of serotonin transporter suggested by three LeuT–SSRI structures. *Nat. Struct. Mol. Biol.* **2009**, *16*, 652–657. [CrossRef] [PubMed]
47. House, H.O.; Koepsell, D.; Jaeger, W. Derivatives of 1, 8-diphenylanthracene. *J. Org. Chem.* **1973**, *38*, 1167–1173. [CrossRef]
48. del Rosario Benites, M.a.; Fronczek, F.R.; Maverick, A.W. Intermolecular hydrogenation of a C C bond during π-cyclopentadienyliron complexation of 1, 8-dichloro-9, 10-dihydro-9, 10-ethenoanthracene. *J. Organomet. Chem.* **1999**, *577*, 24–30. [CrossRef]

49. Lidström, P.; Tierney, J.; Wathey, B.; Westman, J. Microwave assisted organic synthesis—a review. *Tetrahedron* **2001**, *57*, 9225–9283. [CrossRef]
50. Wathey, B.; Tierney, J.; Lidström, P.; Westman, J. The impact of microwave-assisted organic chemistry on drug discovery. *Drug Discov. Today* **2002**, *7*, 373–380. [CrossRef]
51. Gawande, M.B.; Shelke, S.N.; Zboril, R.; Varma, R.S. Microwave-assisted chemistry: Synthetic applications for rapid assembly of nanomaterials and organics. *Acc. Chem. Res.* **2014**, *47*, 1338–1348. [CrossRef]
52. Sasaki, S.; Ishibashi, N.; Kuwamura, T.; Sano, H.; Matoba, M.; Nisikawa, T.; Maeda, M. Excellent acceleration of the Diels-Alder reaction by microwave irradiation for the synthesis of new fluorine-substituted ligands of NMDA receptor. *Bioorganic Med. Chem. Lett.* **1998**, *8*, 2983–2986. [CrossRef]
53. Díaz-Ortiz, A.; Carrillo, J.; Gómez-Escalonilla, M.J.; de la Hoz, A.; Moreno, A.; Prieto, P. First Diels-Alder reaction of pyrazolyl imines under microwave irradiation. *Synlett* **1998**, *1998*, 1069–1070. [CrossRef]
54. Kaplan, F.; Conroy, H. Electronic Effects on the Stereochemistry of the Diels—Alder Reaction1. *J. Org. Chem.* **1963**, *28*, 1593–1596. [CrossRef]
55. Verma, S.M.; Singh, M.D. Structural elucidation with nuclear magnetic resonance spectroscopy. Diels-Alder adducts of 1-aminoanthracene and maleic anhydride: Restricted rotation about the aryl C (1)-N bond and intrinsic asymmetry about the imide (Nsp2-Csp3) system. *J. Org. Chem.* **1977**, *42*, 3736–3740. [CrossRef]
56. Singh, M.D.; Ningombam, A. High stereoselectivity in the Diels-Alder reaction of substituted anthracenes: Reactions of 1-succinimidoanthracene and 1-phthalimidoanthracene with maleic anhydride. *Indian J. Chem.* **2010**, *49*, 789–794. [CrossRef]
57. Schmidt, C.; Sabnis, S.; Schmidt, E.; Taylor, D. Substituent Effects on the Orientation of Diels-Alder Reactions. II. *Can. J. Chem.* **1971**, *49*, 371–374. [CrossRef]
58. Khan, R.; Ningombam, A.; Singh, K.B.; Singh, M.D. Stereoelectronic effects in the Stereoselectivity of the Diels-Alder Reactions: Reactions of Aminoanthracenes with N-phenylmaleimide. *J. Chem. Pharm. Res.* **2012**, *4*, 1532–1538.
59. Chung, Y.; Duerr, B.F.; McKelvey, T.A.; Nanjappan, P.; Czarnik, A.W. Structural effects controlling the rate of the retro-Diels-Alder reaction in anthracene cycloadducts. *J. Org. Chem.* **1989**, *54*, 1018–1032. [CrossRef]
60. Ertl, P.; Rohde, B.; Selzer, P. Fast calculation of molecular polar surface area as a sum of fragment-based contributions and its application to the prediction of drug transport properties. *J. Med. Chem.* **2000**, *43*, 3714–3717. [CrossRef]
61. Lipinski, C.A.; Lombardo, F.; Dominy, B.W.; Feeney, P.J. Experimental and computational approaches to estimate solubility and permeability in drug discovery and development settings. *Adv. Drug Deliv. Rev.* **1997**, *23*, 3–25. [CrossRef]
62. Daina, A.; Michielin, O.; Zoete, V. SwissADME: A free web tool to evaluate pharmacokinetics, drug-likeness and medicinal chemistry friendliness of small molecules. *Sci. Rep.* **2017**, *7*, 42717. [CrossRef]
63. Brenk, R.; Schipani, A.; James, D.; Krasowski, A.; Gilbert, I.H.; Frearson, J.; Wyatt, P.G. Lessons learnt from assembling screening libraries for drug discovery for neglected diseases. *ChemMedChem* **2008**, *3*, 435. [CrossRef]
64. Baell, J.B.; Holloway, G.A. New substructure filters for removal of pan assay interference compounds (PAINS) from screening libraries and for their exclusion in bioassays. *J. Med. Chem.* **2010**, *53*, 2719–2740. [CrossRef] [PubMed]
65. Young, R.C.; Mitchell, R.C.; Brown, T.H.; Ganellin, C.R.; Griffiths, R.; Jones, M.; Rana, K.K.; Saunders, D.; Smith, I.R. Development of a new physicochemical model for brain penetration and its application to the design of centrally acting H2 receptor histamine antagonists. *J. Med. Chem.* **1988**, *31*, 656–671. [CrossRef] [PubMed]
66. Zanger, U.M.; Schwab, M. Cytochrome P450 enzymes in drug metabolism: Regulation of gene expression, enzyme activities, and impact of genetic variation. *Pharmacol. Ther.* **2013**, *138*, 103–141. [CrossRef] [PubMed]
67. Xu, C.; Cheng, F.; Chen, L.; Du, Z.; Li, W.; Liu, G.; Lee, P.W.; Tang, Y. In silico prediction of chemical Ames mutagenicity. *J. Chem. Inf. Modeling* **2012**, *52*, 2840–2847. [CrossRef]
68. Mulliner, D.; Schmidt, F.; Stolte, M.; Spirkl, H.-P.; Czich, A.; Amberg, A. Computational models for human and animal hepatotoxicity with a global application scope. *Chem. Res. Toxicol.* **2016**, *29*, 757–767. [CrossRef]
69. Kalyaanamoorthy, S.; Barakat, K.H. Development of safe drugs: The hERG challenge. *Med. Res. Rev.* **2018**, *38*, 525–555. [CrossRef]
70. Saxena, P.; Zangerl-Plessl, E.-M.; Linder, T.; Windisch, A.; Hohaus, A.; Timin, E.; Hering, S.; Stary-Weinzinger, A. New potential binding determinant for hERG channel inhibitors. *Sci. Rep.* **2016**, *6*, 24182. [CrossRef]

71. Ponte, M.L.; Keller, G.A.; Girolamo, G.D. Mechanisms of drug induced QT interval prolongation. *Curr. Drug Saf.* **2010**, *5*, 44–53. [CrossRef]
72. Siramshetty, V.B.; Nickel, J.; Omieczynski, C.; Gohlke, B.-O.; Drwal, M.N.; Preissner, R. WITHDRAWN—a resource for withdrawn and discontinued drugs. *Nucleic Acids Res.* **2016**, *44*, D1080–D1086. [CrossRef] [PubMed]
73. Li, M.; Ramos, L.G. Drug-induced QT prolongation and torsades de pointes. *Pharm. Ther.* **2017**, *42*, 473.
74. Low, Y.; Uehara, T.; Minowa, Y.; Yamada, H.; Ohno, Y.; Urushidani, T.; Sedykh, A.; Muratov, E.; Kuz'min, V.; Fourches, D. Predicting drug-induced hepatotoxicity using QSAR and toxicogenomics approaches. *Chem. Res. Toxicol.* **2011**, *24*, 1251–1262. [CrossRef] [PubMed]
75. Schuster, D.; Laggner, C.; Langer, T. Why drugs fail-a study on side effects in new chemical entities. *Curr. Pharm. Des.* **2005**, *11*, 3545–3559. [CrossRef] [PubMed]
76. Ames, B.N.; McCann, J.; Yamasaki, E. Methods for detecting carcinogens and mutagens with the Salmonella/mammalian-microsome mutagenicity test. *Mutat. Res./Environ. Mutagenesis Relat. Subj.* **1975**, *31*, 347–363. [CrossRef]
77. Mortelmans, K.; Zeiger, E. The Ames Salmonella/microsome mutagenicity assay. *Mutat. Res./Environ. Mutagenesis Relat. Subj.* **2000**, *455*, 29–60. [CrossRef]
78. Lei, T.; Li, Y.; Song, Y.; Li, D.; Sun, H.; Hou, T. ADMET evaluation in drug discovery: 15. Accurate prediction of rat oral acute toxicity using relevance vector machine and consensus modeling. *J. Cheminformatics* **2016**, *8*, 6. [CrossRef]